Research Article

Journal of Applied Material Science & Engineering Research

Role of Characteristics of External Mechanical Stress and Substrate on the Characteristics of Insulin Aggregates

Indu Sharma and Sudip K Pattanayek*

Department of Chemical Engineering, Indian Institute of Technology, New Delhi, 110016 India

***Corresponding author**
Sudip K Pattanayek, Department of Chemical Engineering, Indian Institute of Technology, New Delhi, 110016 India, Tel: +91 11 26591018; Fax: +91 11 26581120; E-mail: sudip@chemical.iitd.ac.in

Submitted: 26 Jan 2018; **Accepted**: 06 Feb 2018; **Published**: 27 Feb 2018

Abstract

The role of chemical nature of the surface and mechanical stress on the properties of insulin in solution kept in the container is explored. The mechanical stress can be applied in the form of shear force or shaking of content in vials. The process of shear can be continuous or intermittent periodic stoppage of shear. We have observed the secondary structures of insulin present over the surface and in the solution. In addition, we have observed the distribution of insulin size, which arises due to their aggregation in solution.

The properties are found to depend on the processes of applying mechanical force on a solution. The conversions of α-helix to β-sheet for continuous shear, but to intermolecular β-sheet in presence of the interrupted shear are found. The later phenomenon leads to the formation of a bigger particle. The shaking of the content of vials leads to the formation of particles with the higher random coil.

The combined effect of shaking and chemical nature of surface on the aggregates' properties is also observed. The size distribution and secondary structures of aggregates of insulin in solution are strongly dependent on the chemical nature of the surface. These are explained through desorption of the adsorbed protein. The higher rate desorption of protein from lesser hydrophobic surfaces leads to the formation of bigger insulin aggregates.

Keywords: Insulin aggregation, Interrupted shear, Particle size distribution, Secondary structures, Hydrophobic surfaces

Introduction

Stability and the aggregation of a protein is a major concern in process and delivery of a therapeutic protein. It has been reported that both mature and immature protein aggregates are toxic [1]. A small fluctuation in the environmental conditions such as temperature, pH, the composition of medium etc of protein solution leads to the structural change in the native protein, which on turn leads to their aggregation [1-12]. A protein even at a given controlled environment may form aggregates due to mechanical stress (such as shaking orshearing of protein solution) and/or physical and chemical nature of the of thesurface container.

In presence of mechanical stress, one would expect that a protein may behave differently due to the difference in turbulence and local relative motion between protein molecule and medium. The dynamics of a section of the protein is dependent on the shear rate and its duration. It is interesting to see the effect of intermittent shear on the dynamics of the protein. The absence of shear for a given time in the intermittent shear allows segments of protein to relax. These dynamicsis also expected to affect the properties of the protein. It is envisaged that the above dynamics would control the size of aggregates of protein.

In addition, anadsorbed protein over thesurface of the container may contribute towards its aggregationthrough thefollowing mechanism. The adsorbed protein, which has lost its native conformation due to adsorption, may go back into solution. The models describing the adsorption of the protein indicate the presence of above desorption process [13-24]. The desorbed protein with the deformed conformations may accelerate the aggregation process in the bulk solution. Desorption and the subsequent aggregation processes of the protein are expected to be even more rapid in the presence of mechanical disturbance (such as shear). Thus both surface and mechanical stress can accelerate the aggregation process.

A partial verification of the above process was done recently by Pandey et al., who had reported the effect of both hydrophilic and hydrophobic surfaces on the formation of the fibrillar aggregate of human insulin (HI) [25]. The solution of HI was kept into a vial containing desired modified silica beads and agitated at 60 rpm. Subsequently, the kinetics of fibril formation in solution was

measured. It was reported that there was the sudden rise in the aggregate formation after a lag time. It was shown that the silica surface modified with a hydrocarbon containing octyl group has lag time 14 h. The formation of aggregates and their characteristics in the presence of hydrophobic SAMs within the lag time was not explored. In addition, the effect of agitation during this period is required further attention.

In this present study, we have explored the effect of continuous shear, interrupted shear, agitation of the content in presence of added substrates on the size of aggregated human insulin (HI) in solution at a fixed concentration. Continuous shear increases stretching of protein, while the interrupted leads to the formation of slightly bigger aggregate from smaller particles due to the presence of sufficient time to interact with particles at the intermittent stationary condition of the system. The interruption of shear gives protein segments sufficient time to relax to form a stable structure, which is reflected from secondary structures.We have observed the effect of silica beads and modified silica beads with amethyl-terminated group of varying hydrocarbon chain length (i.e. propyl, octyl, and octadecyl) on the properties of aggregates in solution and at the surface. The aggregated particles present in the solution are characterized by particle size and secondary structures of the protein. The HI at the surfaces is characterized by morphology and secondary structures of adsorbed HI.

Materials and Methods

All chemicals like, propyl tri-methoxy silane(PTMS), octyl tri-methoxy silane (OTMS) and octadecyltrichlorosilane (OTCS), anhydrous toluene (99.99% purity) and dimethylformamide were purchased from Sigma-Aldrich. Glass beads of 1 mm diameter, borosilicate glass tube, Human insulin(HI, cat no. I2643) and Tris buffer solution (25mM Tris-HCl, 125 mM NaCl, 2 mM $MgCl_2$, of pH 7.4) were purchased from Sigma-Aldrich. Other reagents, such as methanol, acetone, trichloroethylene (HPLC grade) were used as received from Fisher Scientific. Single-sided polished silicon wafers (p-type, orientation 100) were purchased from Scientific Technologies India.

Cleaning of surfaces

The silicon wafer of the required dimension and glass beads (dia 1mm) were freshly cleaned by using three different solvents trichloroethylene, acetone, and methanol for 5 min in each solvent sequentially. The substrates are dried using a stream of nitrogen with the help of a nitrogen gun. In the next step, substrates were soaked in diluted HF (1:2) for 5 min to remove the native oxide layers. This leads to the formation of H-terminated silicon surfaces. The obtained surfaces were repeatedly washed with de ionized water to remove the organic contaminant. The surfaces were finally treated with methanol and dried under a stream of nitrogen to make stain free substrate. The freshly cleaned substrates were then kept into desiccators to avoid the contamination.

Modification of surfaces

The freshly cleaned substrates were dipped into 1% (v/v) solution of silane coupling agents PTMS, OTMS, and OTCS in anhydrous toluene to obtain propy, octyl and octadecyl groups respectively. The reactions were carried out in a glove box, which was kept at 25°C in nitrogen atmosphere. On completion of the reaction for 12hrs, the modified substrates were cleaned in three sonication bath containing toluene, a mixture of methanol and toluene (1:1) and methanol respectively. After the final stage of cleaning, the modified substrates were kept in the vacuum desiccator, which was prefilled with nitrogen.

Characterization of substrates

The formation of the bond between silica surface and silane coupling agent were characterized by using Fourier Transform Infrared Spectroscopy (FTIR) make Nicolet 6700 spectrophotometer. The processing of the spectra was done using the OMNIC 7.3 software. We have used AFM (make Park Systems Corps.) in the non-contact mode to see the surface morphology before and after modification and Ellipsometer (make SOPRA model GES5E) and Win-Elli-II software for analysis of spectra, to determine the physical characteristics (surface morphology) of the modified surfaces. The contact angle of two test liquids water and methylenediiodide over the modified surfaces was measured using goniometer. This enables us to quantify the characteristics of the surface by its surface energy.

Surface characterization using FTIR

The functional groups on the surfaces were confirmed by the appearance of characteristic peaks corresponding to the specific chemical groups of the modified surfaces in the ATR-FTIR spectra. We took the FTIR spectra of modified surface of silicon wafer recorded in the transmission mode on a Nicolet 6700 FTIR spectrophotometer. The processing of the spectra was done using the OMNIC 7.3 software.

Surface characterization using Goniometer

The sessile drop method was used to measure the contact angle using goniometer (model DSA 100, Kruss, Germany). A drop of 10µl is put on a modified surface kept in a chamber maintained at 25°C temperature. The contact angles are calculated by using inbuilt software, which fits a circle on the obtained drop shape. All reported values herein are the averages of at least nine measurements taken at three different locations on each sample surface. Each sample was preparedin three different batches.

The surface energy was calculated from the measured static contact angles of water and methylene di-iodide over the modified surfaces. The contact angle of a test liquid on the surface is related by the relation to surface energy, of a solid surface (γ_s) and the test liquid (γ_L) [26].

$$(1+Cos\,\theta_i)\gamma_L = 2\left(\left(\gamma_L^d\gamma_s^d\right)^{1/2} + \left(\gamma_L^p\gamma_s^p\right)^{1/2}\right) \qquad (1)$$

Where the superscripts p and d correspond to polar and dispersive components of the surface energy. The reported polar and dispersive components of surface energy (γ_L^p, γ_L^d) of water are 48.87 and 22.3 mJ/m^2 respectively and that of methylene diiodide are 0.03 and 50.8 mJ/m^2 respectively [27]. Using these values and the measured contact angles of two test liquids over the surfaces, we have determined the surface energy of the test surfaces. Assuming zero error in the reported values of polar and dispersive components of the surface energy of test liquids, we have calculated the error in surface energy.

Surface characterization using Ellipsometer

The thickness of modified surfaces, E_d, was measured by using Ellipsometer (make SOPRA model GES5E) and Win-Elli-II software. All thickness measurements were done using the monochromatic light of wavelength 532 nm with the angle of incidence of 70°C. Three

layer models (Si/SiO_2+Silane/air) have been used for determination of the thickness of the oxide layer and SAMs. Data fitting were in good agreement with the Cauchy (n,k) model. The measurements were performed at three different spots of a given sample.

Surface characterization using Atomic Force Microscope

Surface morphology of modified quartz substrates was observed by using AFM (make Park Systems Corps.) in non-contact mode. All measurements were done in ambient condition using silicon-nitride cantilever with typical spring constant of 42N/m (resonance frequency of about 260 kHz in air) using a scan rate of 0.75Hz. The textures obtained from AFM having a size of 1×1 μm were analyzed using XEI 1.8.0 available with the AFM. The morphology of the substrates was quantified by power spectrum density (PSD) analysis and R_{pv}(nm), R_q(nm), R_a(nm), R_z(nm),R_{sk}, and R_{ku}, which are discussed below.

Preparation of Protein Solution

The insulin solution of concentration 1mg/ml was prepared in (10mM) Tris–Buffered Saline, TBS (25 mM Tris–HCl, 125 mM NaCl, 2 mM $MgCl_2$, pH 7.4) solution. The choice of protein concentration is based on its low concentration (30IU) used in the injection vials. We have used the freshly prepared solution.

Shear experiment with Protein Solution

Brookfield DV-III Ultra Rheometer is used to shear the HI solution. 1.5 ml solution of HI was kept in the cup of the rheometer at room temperature (25°C) and the temperature of the system is brought to the desired temperature 40°C. The solution within the viscometer was sheared as required. We note that shear rate is proportion to the rpm of the spindle. The proportionality constant is called the shear rate constant, which depends on the geometry (cone angle and separation of the tip of the cone and plate) of spindle used. CPE 40 spindle of Brook field DV-III was used. For this, the shear rate and rpm are related by the relation, shear rate (s^{-1}) = 7.5×rpm. The sample of the protein solution is taken out time to time to measure the particle size and IR-FTIR spectra. We have compared the particle size and secondary structures of protein solution (1mg/ml) at three different shear rates 600, 1500 and 1875 sec^{-1}, which are corresponding to the rotational speed of spindle 80, 200 and 250 rpm respectively.

Continuous shear and Interrupted shear experiments

In the continuous shear experiment, the spindle rotates at a selected rpm until the desired time or the developed torque is within the measurable limit of the instrument is reached. In the interrupted shear experiment, the protein solution is sheared at a selected rpm continuously for 10 min and subsequently, the rotation of the spindle is made to zero for 10 min. This process is continued till the developed torque is within the measurable limit of the instrument.

Shaking experiment with protein solution

We have placed the 1.5ml borosilicate glass tubes containing 1.0 ml of 1mg/ml insulin solution in a vertical shaker (make Tradevel Scientific Technologies).These tubes are agitated for a pre-decided set time (1hr, 2hrs, 3hrs, 4hrs and 6hrs) at a pre-decided rotational speed (8, 80, 200 250 rpm) at 40°C. We have observed the variation of particle size and secondary structures of protein in the absence of any added surface. The particle size was measured by using dynamic light spectroscopy (discussed below). IR-FTIR was used to determine the secondary structure of the protein (discussed below).

Shaking experiment with protein solution and modified surface

We have observed the effect of the surface by adding 1.0 ml of insulin solution(1mg/ml)into a borosilicate glass tube(surface area ca 4 cm^2) containing 200 mg of glass beads (total surface area of a particle ca 14 cm^2). Four different types of glass beads, namely, unmodified silica beads and modified silica beads with PTMS, OTMS, and OTCS were used separately. Subsequently, the glass tubes were agitated for a required time (1hr, 2hrs, 3hrs, 4hrs and 6hrs) at a predefined rotational speed (8, 80, 200 and 250 rpm) at 40°C. The liquid samples were collected by using micropipette and were analyzed for particle size and secondary structures.

Measurement of Particle Size

The size distribution of the aggregates is determined using particle size analyzer (Malvern zetasizer PSW0085/7.01). A shifted Gaussian curve is given by

$$N_p = y_0 + \frac{A}{\sqrt{\pi/2}\,W_c} exp\left[-2\left(\frac{x-X_c}{W_c}\right)^2\right] \qquad (2)$$

is fitted to the obtained size distribution in Origin Pro8. Here, the fitted parameter X_c is the mean size of the particles, Wc is the width of the distribution and y0 is a constant, indicating the shift of the distribution, which is very close to zero. A low value of W_c is corresponding to the narrow distribution of particles. A typically fitted curve is shown in supplementary doument (figure A1).

Measurement of Secondary structure

We also took the FTIR spectra of protein samples before and after any one of the above process (discussed in section 2.3.6,2.3.7,2.3.8). in the transmission mode on a Nicolet 6700 FTIR spectrophotometer. Ge trough (0039-613) of Thermo Scientific Madison, WI, USA was usedfor the tests using protein solution. The spectra for various cases were collected at the resolution of $4cm^{-1}$ and scan rate 64 for getting a good signal to noise ratio. The spectra of solvent were collected at same instrument conditions. Each sample spectra further processed using OMNIC 7.3 software, for the digital deduction solvent spectra and base line correction and smoothness. The characteristic peak of amide- I band of the proteins, which is due to carbonyl stretching vibrations appears at wave number 1600-1700 cm^{-1} range. The amide-I band region is fitted to Gaussian curves which are the best method to quantify the percentage of protein secondary structure [28]. To find out the multi-peak position, we have done the Fourier self-deconvolution (FSD) of protein amide-I band using OMNIC software. Then quantification of multi component peak areas was done using Gaussian fitting in Origin Pro8 to determine various components of secondary structures namely β-sheet, random coils, α-helix, and β-turn, which appears at wave number ranges 1614-1634cm^{-1}, 1635-1648cm^{-1}, 1650-1658cm^{-1} and 1662-1684 cm^{-1} respectively [28,29]. In addition, the peak bands at 1610, 1614, 1625 and 1685-1698cm^{-1} corresponds to side chain, intermolecular β-strand, intra molecular β-strand and anti parallel β-sheet respectively [30-34]. The sensitivity or confidence of fit can be decided in the least square sense (i.e. by R^2 value) which, is always varying in the range from 0.92-0.99 [28,35]. A typical plot is shown in supplementary document figure A2. We note that we have reported secondary structures as α-helix, β-sheet which includes intra molecular β-sheet and β-turn, random coils (RC) includes a random coil and side chains. In addition, the sum of the proportion of inter molecular β-sheet and anti parallel β-sheet are represented as Iβe.

Results and Discussion

Aggregation of insulin in presence of shear

Continuous Shear

Figure 1a compares the size of aggregated HI and its distribution in solution after continuous shearing of the solution for 4 hours at three different rotational speeds of the spindle (corresponding to different shear rate) at temperature 40°C. The figures also indicate the particles size and their distribution in the originally prepared solution at 25°C. The aggregated particle of HI in Tris buffer solution at 25°C has the mean size 5.6 nm width of distribution 2.4 nm. The mean size is very close to the reported hydrodynamic diameter of HI is 5.8nm.At a higher rotation speed of spindle, there is an increase in particle size with wider particle size distribution [36].

Figure 1b compares the proportion of various secondary structures of HI in solution at the above stated conditions at 40°C and 25°C. The secondary structure analysis shows that the proportion of α-helix, β-sheet, β-turn and random coil content are 54, 6, 20, and 20% respectively for HI at 25°C. This data is very close to the reported data on secondary structures of insulin solution at 25°C in 10mM Trizma [37].

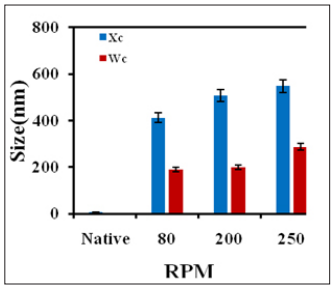

Figure 1(a)

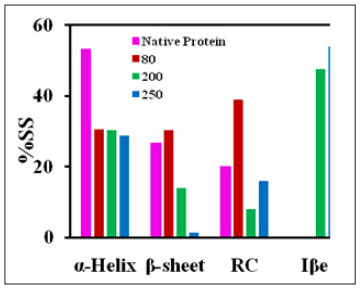

Figure 1(b)

Figure 1: Comparison of characteristics of HI in native state at 25°C and HI in solution after continuous shear at different rotational speeds of spindle for 4 hours at 40°C .(a)Mean Particle size (X_C), distribution span(W_C) and (b)Secondary structure %SS.

Interrupted Shear

Figure 2 compares the size and proportion of various secondary structures at 80rpm with continuous and interrupted shear. The conversion of α-helix to random coil takes place due to shear. On subsequent rest during the interrupted shear experiment, the conversion of the random coil to β-sheet or intermolecular β-sheet takes place. This indicates that interruption gives sufficient time to HI molecules with the random coil segment to form intermolecular β-sheet. This leads to the increase in particle size as shown in figure 2a. We cannot study the effect of surface and shear in the viscometer but can be studied in shaking experiment. Below, we compare the effect of continuous shear and shaking of the vial on the particle size and their characteristics below.

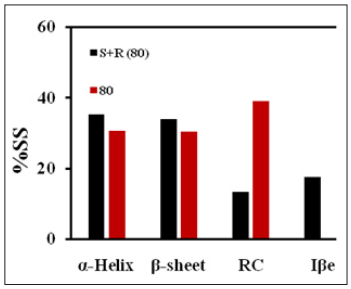

Figure 2(a)

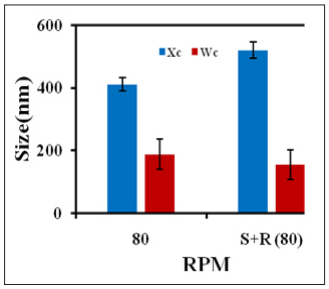

Figure 2(b)

Figure 2: Comparison of the effect of continuous shear and the interrupted shear on the characteristics of HI in Tris buffer solution (conc. 1mg/ml)at rotational speed 80 rpm of spindle for 4 hours at 40°C (a)proportion of Secondary structure %SS and (b) variation in average particle size (X_C) and width of distribution (W_c).

Aggregation of insulin in presence of shaking

Figure 3 shows size and the proportion of various secondary structures of aggregates/particles of HI in solution at 40°C after shaking of vials at different rpm for 6 hours. In general, there is the increase in particle size with increasing rotational speed of vials. Comparing the figure 3a with figure 1a, the mean size of the aggregates is more for shaking than as hear experiment. This is probably due to the higher tearing of bigger particles during a continuous shear experiment in viscometer. It is expected that during shaking process the shear created due to external rotational force(actual shear cannot be quantified) leads to the conversion of α -helix to the random coil in the protein molecules, which is supported by the secondary structure of protein obtained (see Figure 3 b). The figure indicates that there is a considerable amount of random coil, β-sheet, and intermolecular β-sheet. The comparison of secondary structures of insulin obtained for the two cases (Figure 1b and 3b), a considerably higher amount of random coil in particles obtained from shaking experiments was found. The obtained large aggregates with a higher proportion of random coil after shaking experiments are probably the weakly associated, soluble aggregates.

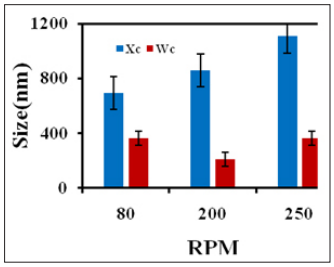

Figure 3(a)

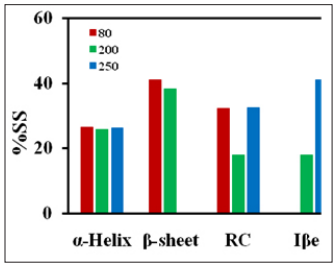

Figure 3(b)

Figure 3: Effect of shaking the vial of HI in Tris buffer solution (conc., 1mg/ml)at various rotational speeds of shaker at 40°C after 6 hours (a)variation inaverage particle size (X_C) and width of distribution (W_c) and (b) proportion of Secondary structure %SS.

Effect of Surface

Characterization of surface

The silicon wafer after modification is analysed to get the characteristics of the modified silica surface. IR-FTIR graphs of surfaces of a silicon wafer with three different modifiers (shown in supplementary figure A3) were analyzed. The regular position of the peaks of various groups in IR-FTIR spectra and the location of appearance of the corresponding peak in IR-FTIR of PTMS, OTMS, and OTCS are listed in table 1. C-H asymmtric stretch can be found in two locations: medium intensity 2920-2970 cm^{-1} and sharp intensity 1430-1470 cm^{-1}. C-H sym. stretch can be found in two locations: sharp intensity 2850-2880 cm^{-1} and medium intensity 1370-1390 cm^{-1} [17,21,39,40]. The intensity of peaks corresponds to high-intensity C-H sym (2850-2880 cm^{-1}) and C-H a sym [39-43]. Stretch (1430-1470 cm^{-1}) increases and the location of peaks shift to a higher value as carbon number of the modifier increases (see figure A3). The high intensity is corresponding to the good packing of hydrocarbons [44-46]. From this data, we conclude that the packing of hydrocarbons in PTMS is random while in OTMS and OTCS the packing is reasonably good [44].

Table 1: Chemical functional groups corresponding to SAMs and their position in FTIR Spectra .

Functional group	Literature Peak Position(cm-1)	PTMS	OTMS	OTCS
C-H asym. stretch	2920-2970 [17,18]	2972	2923	2934
C-H sym. stretch	2850-2880 [17-21]	2852	2857	2867
C-H asym. stretch	1430-1470 [17-21]	1428	1462	1472
C-H sym. stretch	1370-1390 [17-21]	1383	1382	1378
O-Si-C	1080-1110 [17,18]	1082	1089	1087

The various characteristic parameters of modified surfaces, which were determined by using AFM, ellipsometer, and goniometer, are shown in Table 2. The AFM images of the various modified surfaces were analyzed to obtain the roughness parameters: peak to valley distance (Rpv), and average roughness, Ra. From the data of pure silica and modified surfaces, we can state that the increased chain length of SAMs leads to increase in roughness and ellipsometric thickness of modified surfaces.

Table 2: Surface Energy and physical characteristics of SAMs

SAMs	Ra (nm)	Rpv (nm)	E_d (nm)	Water (Θ)	MI (Θ)	γ^p	γ^d	γtotal (mJ/m^2)
PTMS	0.30	0.51	1.18	90.6	48	3.02	32.06	35.04±1.0
OTMS	0.54	0.61	1.41	103	49	2.4	23.2	25.6±0.7
OTCS	1.7	2.3	2.6	107	68	0.5	23.4	23.9±1.3

The contact angles of two different liquids namely water and methylene diiodide (MI) are used to determine the surface energy using the procedure as discussed earlier. The measured contact angles, polar and dispersive part and the total surface energy are reported inTable2. The lower values of polar and total surface energies are observed for a SAMs with a longer hydrocarbon chain.

Effect of silica beads on aggregated particles in solution

The effect of unmodified silica on the size and secondary structure of aggregates of HI in solution is shown in Figure 4. Bigger aggregates were found to appear at a longer time of shaking and a higher rotational speed of shaker. The comparison of the secondary structures of protein aggregates in the solution obtained after 6 hours of shaking due to the presence of silica particles at two different rotational speeds are shown in figures 4b and 4c. The presence of surface leads to the formation of a higher proportion of β-sheetat 8rpm and intermolecular β-sheet at 80rpm. A higher rotational speed leads to the formation of aggregated molecules (intermolecular β-sheet) at thepresence of thesurface.

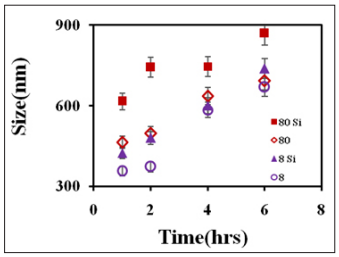

Figure 4(a)

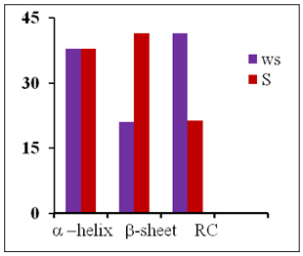

Figure 4(b)

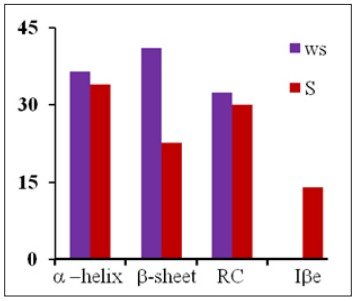

Figure 4(c)

Figure 4: Effect of silica particles on characteristics of aggregates of HI in Tris buffer solution (conc., 1mg/ml)at various agitation speeds at 40°C (a) average particle size (X_c) at various rotational speed in presence (solid symbol) and absence (unfilled symbol) of silica particle (b) Proportion of secondary structure of the aggregates in solution in absence (ws) and presence (S) silica particle at 8rpm (c) Proportion of secondary structure of the aggregates in solution in absence (ws) and presence (S) silica particle at 80rpm

Effect of modified silica beads on aggregated particles in solution

In Figure 5a, we have compared particle size of the aggregates in solution after 6 hours of shaking in presence of three different modified silica particles at two different rotational speeds 8 and 80 rpm. The figure indicates that at a given rotational speed, the average size of aggregated HI particles in solution is independent on the surfaces except for PTMS surface. In the event of similar mechanical stress, it is envisaged that desorbed HI from the surface may control the aggregated particles. The higher average HI particle size in presence of PTMS surface indicates that desorption of HI is considerable from the surface (PTMS). The desorbed HI from PTMS surface continues to grow bigger due to a higher proportion of random coil (see below). The desorption of adsorbed HI is lesser from the highly hydrophobic surfaces (OTMS and OTCS), probably due to stronger binding with the surface. The secondary structures of the aggregates in the above cases are compared in figures 5b and 5c. The transformations of α-helix to β-sheet or intermolecular β-sheetvia random coil were observed at both the rotational speeds. The more amount of intermolecular β-sheetwas observed at 80rpm. In general, a higher amount of intermolecular β-sheet was observedin the solution obtained in presence of the most hydrophobic surface. This indicates that the presence of a longer chain hydrocarbon over the adsorbing surface control the secondary structures of the desorbed HI molecules. The proportion of change in secondary structures due to adsorption at the surface may shed light on desorption process and discuss subsequently.

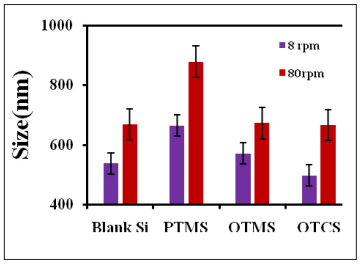

Figure 5(a)

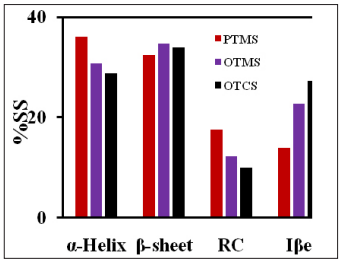

Figure 5(b)

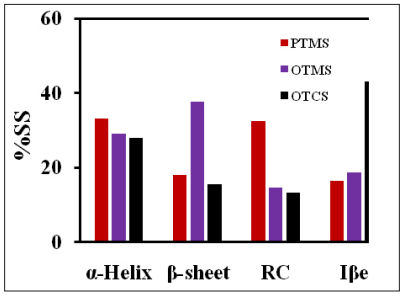

Figure 5(c)

Figure 5: Effect of various modified silica particles on the characteristics of aggregated HI in solution in tris buffer solution at various rotational speeds at 40°C after 6 hours (a) Variation inaverage particle size (XC)(b) Proportion of various components of secondary structure of the HI aggregates in solution due to 8rpm (c) Proportion of secondary structure in the aggregates in solution due to 80 rpm

Morphology of HI after 6 hrs adsorption over modified silicon wafer

We have obtained the AFM images of the insulin adsorbed surfaces as shown in supplementary Figure A4. The figuresare analyzed to obtain R_a and R_{pv}. Figure 6 compares R_a and R_{pv} values of various substrates before and after adsorption for 6 hours. The roughness of OTCS modified surface is highest among the SAMs modified surfaces and among the adsorbed HI over SAMs. A higher adsorption of protein is assisted by two factors, a very high hydrophobicity, and roughness. In Figure 7, we have compared the secondary structures of adsorbed protein over various surfaces. The appearance of intermolecular β-sheet secondary structure of adsorbed proteins on the highly hydrophobic surfaces.

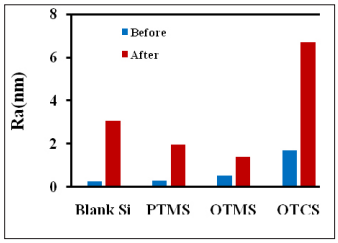

Figure 6(a)

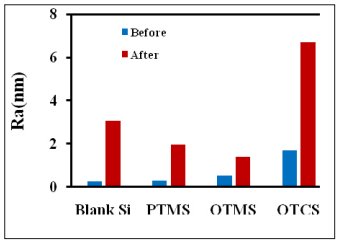

Figure 6(b)

Figure 6: Variation of surface roughness of various modified surfaces and the corresponding surfaces with adsorbed insulin obtained at 80 rpm, 40°C, 1mg/mlHI concentration and 6hrs(a) Ra and (b) Rpv

The secondary structures of HI on PTMS surface indicates that there is a considerable amount of protein with random coil and α helix. On the other hydrophobic surfaces, the protein with a strikingly high amount of intermolecular β-sheet secondary structure are present. In fact, it is observed that a high hydrophobic surface has a very high intermolecular β-sheet over it. Due to the intermolecular binding among the HI molecules over the hydrophobic surfaces, the desorption of HI is very less.

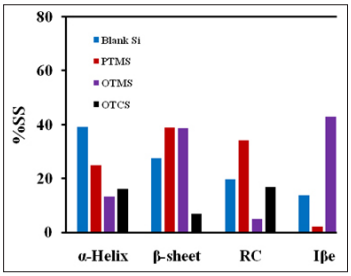

Figure 7: Secondary structure of adsorbed HI on different surfaces after at 80 rpm, 40°C, 1mg/ml and 6hrs

Discussion

Effect of shear

In presence of continuous shear, the conversion of α-helix to other secondary structures depends on the shear rate. At 80rpm, the conversion of α-helix to β-sheet and the random coil is dominating. The similar conversion of α-helix to β-sheet due to shear is already reported in the literature [38]. However, at a higher rotation speed, the conversion of α-helix to intermolecular β-sheet is predominant. It is reported using molecular dynamic simulations that β-sheet has lower potential energy than α-helix at a temperature called transition temperature [47]. The shear force is expected to make the transition of the helix to the random coil and subsequently to α structure easily. A schematic of inter-conversion in the energy landscape of the four major secondary structures is shown in Figure 8. The diagram indicates that α-helix to β-sheet conversion passes through random coil configuration, which subsequently may convert to α-sheet or intermolecular α-sheet. The potential energy difference among various structures is very small. It is expected that random coil of two or more neighbouring protein molecules can interact and subsequently form intermolecular α-sheet. The presence of a higher intermolecular α-sheet at a higher spindle rotational speed (figure 1b) is justifying the transformation to intermolecular α-sheet. This transformation is expected to be more in the case of interrupted shear, as the interruption allows molecules sufficient time to bind among the molecules.

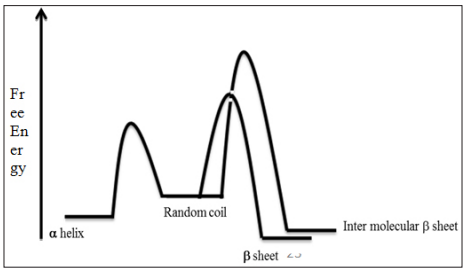

Figure 8: Schematics of transformation of various secondary structures of insulin in Tris buffer solution (conc., 1mg/ml)at 80 rpm at 40°C

Effect of shaking

The shaking of vials, which is usually present in the handling of protein, causes a relative movement of the layer of a fluid over another (shear). The relation between shaking and shear is dependent on the system [48]. It is difficult to relate the two for our system due to aggregation of the protein. Researchers have found the effect of shaking of aggregation of the protein in many cases, see for example references [25,49-53]. Researchers reported the effect additives on the mechanism of aggregation of insulin, which follows a sigmoidal curve. We have not come seen any report on comparing the shear and shaking of a solution containing protein. We have compared the shaking and shearing experiments through the distribution of aggregates size and secondary structures of proteins (compare Figure 1 and Figure 3).

Surface of surface

Effect of interfaces has been explored in various previous studies [25, 50,51]. Reports suggest that the presence interfaces triggers the aggregation at a fixed agitation speed. In addition, the chemical nature of the surface plays an important role in the aggregation. Here

we report thepresence of extra surface and agitation speed increses the size of aggregate and their distribution (figure 4).

To understand the interrelation between secondary structures of protein in solution and at the surfaces, we have compared α helix and total β-component (sum of β-sheet, β-turn, anti-parallel β-sheet, intramolecular and intermolecular β-sheets) them in Figure 9. It is observed that at 8 rpm, the solution and the surface has same composition for given substrate. On increasing the rotational speed, the proportion of alpha helix at the surface is lower than alpha helix proportion of HI in solution. It is well known that the shear rate at the solid surface is the highest. The high shear rate has changed the alpha helix secondary structure to α structures. The figure 9b indicates that the HI at 80 rpm condition has much higher amount of β structures at a given surface. We note that alpha helix of α-content content in solution are dependent on the chemical nature of surface. The insulin over the PTMS surface has a higher amount of random coil structure, which aids to desorption of HI into the solution. The desorbed insulin can grow into bigger size (see Figure 5a), which has good amount random coil in its structure. The appearance of random structure of HI over PTMS is due to the random structure of PTMS molecules over silica surface, which is confirmed from IR-FTIR spectra discussed in earlier section.

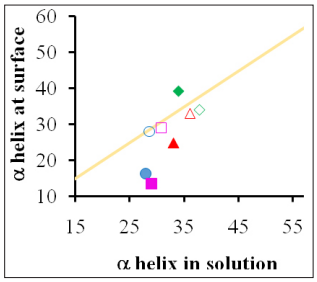

Figure 9(a)

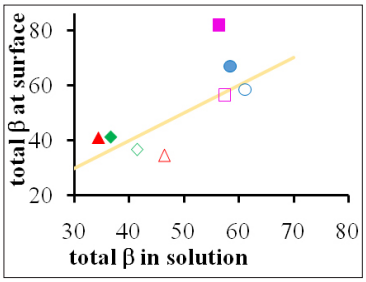

Figure 9(b)

Figure 9: Comparison of secondary structures of HI at surfaces and equilibrium insulin in solution (a) α helix and (b) total amount β sheet (colour code: green:silica, red: PTMS, pink:OTMS, blue:OTCS) at different conditions 8 (empty symbols) and 80 (filled symbols) rpm. The line indicates the 1: 1 line secondary structres in solution and at surface.

Conclusion

It is well-known fact that the mechanical stress such as shear, shaking, the presence of surfaces in solution can lead to aggregation of insulin. We have compared two different methodologies shear experiments: one with continuous shear and another with interrupted shear. The interrupted shear leads to the formation of bigger particle size of HI with more proportion of intermolecular β-sheet in solution. Comparing shear with shaking experiments, a considerable higher size of insulin particles and the particles with higher random coil were observed for the latter case.

The presence of surfaces during shaking experiments leads to the formation of larger size particles of HI with a higher amount of total β content. This is explained through desorption of the adsorbed insulin, which has the relatively higher amount of β content than the native protein. The structure of desorbed HI controls the subsequent aggregation process. It was found for all the surfaces of our studies.

The particle size of insulin in presence of surfaces is independent of the surfaces used, except PTMS surface. The presence of PTMS surface leads to the formation of aggregates of higher mean size with a more random coil in its secondary structure. It is observed that the amount of α-helix in insulin in solution strongly dependent on the chemical nature of the substrate and almost independent on the used experimental shaking speeds.

Acknowledgement

The authors would like to thank SERB, DST, Ministry of Science and Technology (Sanction number SB/S3/CE/086/2013) and Department of Biotechnology (Sanction number BT/COE/34/SP15097/2015) for their financial support for this work.

References

1. Zhu YJ, Lin H, Lal R (2000) Fresh and nonfibrillar amyloid β protein (1–40) induces rapid cellular degeneration in aged human fibroblasts: evidence for AβP-channel-mediated cellular toxicity. FASEB 14:1244-1254.
2. Rathore AS, Joshi V, Yadav N, Pattanayek SK (2013) Refolding of biotech therapeutic proteins expressed in bacteria: review. J Chem Technol Biotechnol 88: 1794-1806.
3. Wei W, Christopher RJ (2010) Aggregation of Therapeutic Proteins. Wiley: Hoboken, New Jersey, USA.
4. Morris AM, Watzky MA, Finke RG (2009) Protein Aggregation Kinetics, Mechanism, and Curve-Fitting: A Review of the Literature. Biochim Biophys Acta 1794: 375-397.
5. Chen S, Lau H, Brodsky Y, Kleemann GR, Latypov RF (2010) The Use of Native Cation-Exchange Chromatography to Study Aggregation and Phase Separation of Monoclonal Antibodies. Protein Sci 19: 1191-1204.
6. Manning MC, Chou DK, Murphy BM, Payne RW, Katayama DS (2010) Stability of Protein Pharmaceuticals: An Update. Pharmaceutical Research 27: 544-575.
7. Varughese MM, Newman J (2012) Inhibitory effects of arginine on the aggregation of bovine insulin. J Biophys 2012: 548-552.
8. Frieden C (2007) Protein Aggregation Processes: In Search of the Mechanism. Protein science : a publication of the Protein Society 16: 2334-2344.
9. Van der Linden E, Venema P (2007) Self-Assembly and Aggregation of Proteins. Curr Opin Colloid In 12: 158-165.
10. Gabrielson JP, Arthur KK (2011) Measuring Low Levels of Protein Aggregation by Sedimentation Velocity. Methods 54: 83-91.
11. Kahook MY, Liu L, Ruzycki P, Mandava N, Carpenter JF, et al. (2010) High-molecular-weight aggregates in repackaged bevacizumab. Retina 30: 887-892.
12. Ferrara N, Hillan KJ, Novotny W (2005) Bevacizumab (Avastin), a Humanized Anti-VEGF Monoclonal Antibody for Cancer Therapy. Biochem Biophys Res Comm 333: 328-335.
13. Pandey LM, Le Denmat S, Delabouglise D, Bruckert F, Pattanayek SK, et al. (2012) Surface Chemistry at the Nanometer Scale Influences Insulin Aggregation. Coll Sur B: Biointer 100: 69-76.
14. Rabe M, Verdes D, Seeger S (2011) Understanding protein adsorption phenomena at solid surfaces. Adv Colloid Inter Sci 162: 87-106.
15. Wahlgren M, Elofsson U (1997) Simple models for adsorption kinetics and their correlation to the adsorption of β-lactoglobulin A and B. J Colloid Inter Sci 188: 121-129.
16. Wertz CF, Santore MM (2002) Adsorption and reorientation kinetics of lysozyme on hydrophobic surfaces. Langmuir 18: 1190-1199.
17. Schaaf P, Talbot J (1989) Surface exclusion effects in adsorption processes. J Chem Phy 91: 4401-4409.

18. Schaaf P, Voegel JC, Senger B (2000) From random sequential adsorption to ballistic desorption: a general view of irreversible deposition processes. J Phy Chem B 104: 2204-2214.
19. Schaaf P, Talbot J (1989) Kinetics of random sequential adsorption. Phy Rev Lett 62: 175.
20. Daly SM, Przybycien TM, Tilton RD (2003) Coverage-dependent orientation of lysozyme adsorption on silica. Langmuir 19: 3848-3857.
21. McGuire J, Wahlgren MC, Arnebrant T (1995) Structural stability effects on the adsorption and dodecyltrimethylammonium bromide-mediated elutability of bacteriophage T4 lysozyme at silica surfaces. J Colloid Inter Sci 170: 182-192.
22. Krisdhasima V, McGuire J, Sproull R (1992) Surface hydrophobic influence on β-lacto globulin adsorption kinetics. J Colloid Inter Sci 154: 337-350.
23. McGuire J, Krisdhasima V, Wahlgren MC, Arnebrant T (1995) Comparative adsorption studies with synthetic, structural stability and charge mutants of bacteriophage t4 lysozyme. in: proteins at interfaces ii: fundamentals and applications, American Chemical Society, Washington, DC.
24. Rabe M, Verdes D, Zimmermann J, Seeger S (2008)Surface organisation, and cooperativity during nonspecific protein adsorption events. J Phys Chem B 112: 13971-13980.
25. Pandey LM, Denmat SLe, Delabouglise D, Bruckert F, Pattanayek SK, et al. (2012) Surface chemistry at the nanometer scale influences insulin aggregation. Colloid Surface B 100: 69-76.
26. Sharma I, Pattanayek SK (2017)Effect of surface energy of solid surfaces on the micro-and macroscopic properties of adsorbed BSA and lysozyme. Biophys Chem 226: 14-22.
27. Rozlosnik N, Gerstenberg MC, Larsen NB (2003)Effect of solvents and concentration on the formation of a self-assembled monolayer of octadecylsiloxane on silicon (001). Langmuir 19: 1182-1188.
28. Yu P (2005) Multicomponent peak modeling of protein secondary structures: comparison of gaussian with lorentzian analytical methods for plant feed and seed molecular biology and chemistry research. Applied Spectroscop. 59:1372-1380.
29. Kong J, Yu S (2007) Fourier transform infrared spectroscopic analysis of protein secondary structures, Acta Biochim Biophy Sin, 39: 549-559.
30. Bramanti E, Ferrari C, Angeli V, Onor M, Synovec RE (2011) Characterization of bsa unfolding and aggregation using a single-capillary viscometer and dynamic surface tension detector. Talanta 85: 2553-2561.
31. Byler DM, Susi H (1986) Examination of the secondary structure of proteins by deconvolved FTIR spectra. Biopolymers 25: 469-487.
32. Byler DM, Susi H (1986) Resolution-enhanced fourier transform infrared spectroscopy of enzymes. Methods in enzymology 130: 290-311.
33. Surewicz WK, Mantsch HH (1988) New insight into protein secondary structure from resolution-enhanced infrared spectra. Biochim Biophys Acta -Protein Struct Molecul Enzym 952: 115-130.
34. Byler DM, Susi H (1983) Protein structure by Fourier transform infrared spectroscopy: second derivative spectra. Biochem Biophys Res Comm 115: 391-397.
35. Chittur KK (1998) FTIR/ATR for protein adsorption to biomaterial surfaces. Biomaterials 19: 357-369.
36. Hvidt S (1991) Insulin association in neutral solutions studied by light scattering. Biophys Chem 39: 205-213.
37. Melberg SG, Johnson WC (1990) Changes in secondary structure follow the dissociation of human insulin hexamers: a circular dichroism study. Proteins: Struct Func Bioinfor 280-286.
38. Webster GT, Dusting J, Balabani S, Blanch EW (2011) Detecting the early onset of shear-induced fibril formation of insulin In situ. J Phys Chem B 115: 2617-2626.
39. Pandey LM, Pattanayek SK (2011) Hybrid surface from self-assembled layer and its effect on protein adsorption. Appl Surf Sci 257: 4731-4737.
40. Clare BH, Abbott NL (2005) Orientations of nematic liquid crystals on surfaces presenting controlled densities of peptides: amplification of protein-peptide binding events. Langmuir 21: 6451-6461.
41. Parikh AN, Allara DL, Azouz IB, Rondelez F (1994) An intrinsic relationship between molecular-structure in self-assembled n-alkylsiloxane monolayers and deposition temperature. J Phys Chem 98: 7577-7590.
42. Allen GC, Sorbello F, Altavilla C, Castorina A, Ciliberto E (2005) Macro-, micro- and nano-investigations on 3-aminopropyltrimethoxysilane self-assembly-monolayers. Thin. Solid. Films 483: 306-311.
43. Aissaoui N, Bergaoui L, Landoulsi J, Lambert JF, Boujday S (2012) Silane layers on silicon surfaces: mechanism of interaction, stability, and influence on protein adsorption. Langmuir 28: 656-665.
44. Janssens M, Gooris GS, Bouwstra JA (2009) Infrared spectroscopy studies of mixtures prepared with synthetic ceramides varying in head group architecture: coexistence of liquid and crystalline phases. BBA-Biomembranes 1788: 732-742.
45. Chan ECY Li, Chalmers J, Griffiths P (2010) Applications of vibrational spectroscopy. Food Sci 1: 128.
46. Brockman JM, Wang Z, Notter RH, Dluhy RA (2003) Effect of hydrophobic surfactant proteins SP-B and SP-C on binary phospholipid monolayers: II. Infrared external reflectance-absorption spectroscopy. Biophys J 84: 326-340.
47. Ding F, Borreguero JM, Buldyrey SV,Stanley HE, Dokholyan NV (2003)Mechanism for the α-helix to β-hairpin transition. Proteins: Struct Func Gene 53: 220-228.
48. Giese H, Klockner WC, Pena E, Galindo S, Lotter K, et al. (2014) Effective shear rates in shake flasks. Chem Engg Sci 118: 102-113.
49. Malik R,Roy I (2011) Probing the mechanism of insulin aggregation during agitation.Int. J. Phar. 413: 73-80.
50. Li S, Leblanc RMJ (2014) Aggregation of insulin at the interface. J Phy Chem B 118: 1181-1188.
51. Frachon T, Bruckert FQ, Masne Le, Monnin E, Weidenhaupt M (2016)Insulin aggregation at a dynamic solid–liquid–air triple interface. Langmuir 32: 13009-13019.
52. Nault L, Guo P, Jain B, Brechet Y, Bruckert F, Weidenhaupt M (2013) Human insulin adsorption kinetics, conformational changes and amyloidal aggregate formation on hydrophobic surfaces. Acta Biomat 9: 5070-5079.
53. Gong H, He Z, Peng A, Zhang X, Cheng B, Sun Y, Zheng L, Huang K (2014) Effects of several quinones on insulin aggregation. Sci Reports 4: 5648.